

1 An exploratory modelling study on sediment transport  
2 during the Zanclean flood of the Mediterranean

3 R. Periañez\*, J.M. Abril†  
Dpto. Física Aplicada I  
ETSIA, Universidad de Sevilla  
Ctra. Utrera km 1, 41013-Sevilla, Spain

4 D. Garcia-Castellanos‡  
Instituto de Ciencias de la Tierra Jaume Almera, CSIC  
Solé i Sabarís s/n  
08028-Barcelona, Spain.

5 F. Estrada§ G. Ercilla¶  
Instituto de Ciencias del Mar, CSIC  
Passeig Marítim de la Barceloneta 37-49  
08003-Barcelona, Spain

6 April 11, 2018

7 **Abstract**

8 A nearly 400 km long erosion channel through the Strait of Gibraltar has been  
9 interpreted as evidence for a catastrophic refill of the Mediteranean at the end of  
10 the Messinian salinity crisis, 5.33 milion years ago. This channel extends from  
11 the Gulf of Cadiz to the Algerian Basin and implies the excavation of ca. 1000  
12 km<sup>3</sup> of Miocene sediment from the Alboran Basin and bedrock from the Strait of  
13 Gibraltar. The fate of these eroded materials remains unknown. In a first attempt  
14 to predict the distribution of those flood deposits, here we develop a numerical  
15 model to simulate the transport of material eroded from the Strait of Gibraltar. It  
16 is a Lagrangian model based upon standard sediment transport equations able to  
17 simulate suspended and bed-load sediment transport. Water circulation during the

---

\*rperianez@us.es

†jmabril@us.es

‡d.g.c@csic.es

§festrada@icm.csic.es

¶gemma@icm.csic.es

flood has been obtained from a hydrodynamic model of the whole Mediterranean Sea previously developed by the authors and applied to the Zanclean flood. Five particle sizes have been considered for suspended load and three for bed-load transport. Areas of sediment deposition in the Mediterranean Sea have been determined. In the case of suspended load, these are related to hydrodynamic conditions: areas sheltered from the jet of incoming water by local topography and areas where water currents abruptly decrease due to a sudden increase in water depth. In the case of bed-load transport, sediments follow water streamlines and deposits are much more localized than in the case of suspended-load. Single channel seismic records have also been analyzed to identify and characterize flood-related deposits in the eastern Alboran Sea.

**Keywords:** numerical model, suspended load, bed load, deposition, Mediterranean Sea, Zanclean flood

## 1 Introduction

The closure of the Guadalhorce and Rifian gateways (Fig. 1A), which were the connections between the Atlantic Ocean and the Mediterranean Sea before the Messinian (7.2-5.3 Ma), limited the water exchange and led to the “Messinian Salinity Crisis” (MSC). During the MSC (5.96-5.33 Ma), the whole Mediterranean basin was at least partially isolated from the world ocean (Hsü et al., 1973; Ryan, 2009; Roveri et al., 2014; García-Castellanos and Villaseñor, 2011), resulting in widespread salt precipitation and a decrease in the Mediterranean sea level at the kilometer scale. Following this extended interpretation, the Mediterranean Sea was later abruptly refilled during the so-called Zanclean flood. Discussions persists regarding the timing and the triggering mechanism of this process (see the review by Roveri et al., 2014). García-Castellanos et al. (2009) reported strong evidence for a deep incision channel along the Gibraltar Strait from boreholes and seismic data generated in the frame of the Africa-Europe tunnel project. The erosion channel has a length of more than 400 km from the Gulf of Cadiz (Esteras et al., 2000) to the Alboran Sea (Estrada et al., 2011) -see Fig. 1 for locations of geographic names mentioned in the text-, with a varying width (2 to 8 km) and depth (200 to 600 m). García-Castellanos et al. (2009) postulated that the observed channel was excavated by the Zanclean flood

(thus it is denoted as the Zanclean Channel) and applied a one-dimensional model which indicated that 90% of the water was transferred towards the Mediterranean in a short period, ranging from few months to two years. These results were later confirmed through computational fluid dynamics simulations carried out using a two-dimensional depth-averaged model of the whole Mediterranean Sea (Periáñez and Abril, 2015).

More recently, Abril and Periáñez (2016) carried out new simulations in which an erosion model was included within the fluid dynamics model, allowing to estimate how the erosion channel was excavated through time. Thus, the main geological features of the Zanclean Channel, including a sill depth of a few hundred meters at Gibraltar, could be understood from a scenario of catastrophic flooding of the Mediterranean with initial conditions consisting of a wide sill surpassed by a thin water layer. In that work, the modelled scenario which better fulfills the known constraints leads to a peak water flow of  $70 \text{ Sv}^1$ . This value is achieved when the water level at the Mediterranean is only about 170 m below the Atlantic level, as will be discussed in section 2.2. At this stage, the height of the water column in the Alboran Sea is high enough to ensure small bottom shear stresses and negligible erosion, but the giant jet of water crossing the Strait of Gibraltar produces in this area bottom shear stresses of  $1,8 \times 10^4 \text{ Pa}$  and incision rates of 1,4 m/day (see their Figs. 5, 9 and 10). Accounting for the size of the area undergoing erosion and the indicated incision rate, the amount of removed material should have been of the order of  $1 \text{ km}^3$  per day. According to these authors, for earlier stages of the flood, during which the Alboran Sea remained almost dessicated, the Atlantic inflow would have remained confined within the path of the Zanclean Channel, releasing its associated sediment load into the Algerian Basin.

Thus, the remaining open question is: where the ca.  $1000 \text{ km}^3$  of seafloor eroded by the flood was deposited? Answering this question may lead to an independent validation (or refutation) of the catastrophic flood hypothesis. Sediments were eroded due to

---

<sup>1</sup>1 Sv= $10^6 \text{ m}^3/\text{s}$

the intense currents existing in the Strait during the flood and transported towards the Mediterranean; where they had to be deposited when currents were not strong enough to keep them in movement. Consequently, large deposits of sediments coming from the Strait of Gibraltar should be present somewhere in the Mediterranean Sea. The purpose of this work is to investigate, using a sediment transport model, where sediments could have been deposited. Single channel seismic records (320 cubic inch) have also been analyzed to identify and characterize flood-related deposits in the eastern Alboran Sea. Because we use a bathymetry reconstruction from the present-day bathymetry as a proxy for the Miocene Mediterranean, model results must be interpreted with caution. The aim of the present paper is to show the general relationships between bathymetry and the deposition of the erosional products.

The model, which is based on standard formulations of sediment transport processes, is described in the next section. Later, results are presented and discussed.

## 2 Model description

A sediment transport model requires water depths and currents over the considered domain. These are generally produced by a hydrodynamic model. The hydrodynamic model is the one described in Periañez and Abril (2015), as applied to simulate the Zanclean flood of the Mediterranean. It is a two-dimensional depth averaged model. The sediment transport model and the hydrodynamic setup for simulations are described in the following subsections.

### 2.1 Sediment transport

The model is able to simulate the transport of particles in suspension (suspended load) and particles which are travelling immediately above the seabed (bed load), which occurs for the larger grain sizes. Equations for each transport mode are presented separately.

98 The sediment transport model works on a Lagrangian framework. Thus, the paths of  
 99 particles are followed along the simulation in both transport modes. The Lagrangian  
 100 approach has been adopted to avoid numerical problems (like large numerical diffusion)  
 101 which would arise from the extremely high flow velocities during the Zanclean flood if an  
 102 Eulerian model were used.

### 103 **2.1.1 Suspended load**

104 Sediment particles are released in the Strait of Gibraltar, just downstream the sill and  
 105 homogenously distributed over the transversal section of the Strait. Then they are trans-  
 106 ported by water currents and mixed by turbulence. Particles fall according to a settling  
 107 velocity which depend on their size and are deposited on the seabed once they reach the  
 108 bottom and if the bed stress is lower than a critical deposition stress. This critical stress  
 109 depends on the particle size as well. Local bed stresses are provided by the hydrodynamic  
 110 model as explained below.

111 Advective horizontal transport is calculated from the following equation for each par-  
 112 ticle:

$$\frac{d\mathbf{r}}{dt} = \mathbf{q} \quad (1)$$

113 where  $\mathbf{r}$  is the position vector of the particle and  $\mathbf{q}$  is the current vector at the particle  
 114 position, solved in components  $u$  and  $v$  (east-west and south-north directions respectively).  
 115 Note that the hydrodynamic model is two-dimensional, thus it does not calculate a vertical  
 116 water velocity,  $u$  and  $v$  being depth-averaged. Nevertheless, the suspended sediment  
 117 transport model is fully three-dimensional: horizontal and vertical movements of particles  
 118 are calculated as described below.

119 An additional horizontal advective velocity vector  $(\partial K_h/\partial x, \partial K_h/\partial y)$  is included to  
 120 avoid the accumulation of particles in regions of low horizontal diffusivity (Proehl et al.,  
 121 2005).  $K_h$  and  $K_v$  are, respectively, the horizontal and vertical eddy diffusivities, which

are deduced from water circulation. In particular, the Smagorinsky's scheme (Cushman-Roisin and Beckers, 2011) has been adopted to describe the horizontal diffusivity:

$$K_h = \Delta x \Delta y \sqrt{\left(\frac{\partial u}{\partial x}\right)^2 + \left(\frac{\partial v}{\partial y}\right)^2 + \frac{1}{2} \left(\frac{\partial u}{\partial y} + \frac{\partial v}{\partial x}\right)^2} \quad (2)$$

where  $\Delta x$  and  $\Delta y$  are the grid cell sizes in the east-west and south-north directions respectively. Both values are 4 minutes of arc in the present application. The approach used by Lane (2005) in a Lagrangian sediment transport model has been adopted for the vertical diffusion coefficient:

$$K_v = k|\mathbf{q}|H \quad (3)$$

where  $k = 0.0025$  is the bed friction coefficient used in the hydrodynamic model and  $H$  is the local water depth.

Particle settling is evaluated according to the following equation:

$$\frac{dz}{dt} = w_s \quad (4)$$

where  $w_s$  is the settling velocity for the corresponding particle size (measured positive downwards) and  $z$  is the vertical location of the particle (measured downwards from the local sea surface). When a particle falls on the seabed, it is deposited if the local bed stress is lower than a critical deposition stress,  $\tau_{cd}$ , above which deposition does not occur. If deposition is not occurring, the particle is reflected back to the water column. It must be noted that the erosion process itself is not modelled: only the paths of particles released in the Strait of Gibraltar are calculated and new particles are not incorporated to the water column from other regions. This has been done since we are interested in the fate of particles eroded from the Strait of Gibraltar.

A stochastic method is used to describe turbulent mixing. Thus, it is considered that the maximum size of the horizontal step given by the particle,  $D_h$ , is (Proctor et al., 1994;

142 Hunter, 1987; Periañez and Elliott, 2002):

$$D_h = \sqrt{12K_h\Delta t} \quad (5)$$

143 in the direction  $\theta = 2\pi RAN$ , where  $RAN$  is a random number between 0 and 1.  $\Delta t$  is  
144 the time step used to integrate the model. This equation gives the maximum size of the  
145 step. In practice, it is multiplied by  $RAN$  to obtain the real size at a given time and for  
146 a given particle. Similarly, the maximum size of the vertical step is (Proctor et al., 1994;  
147 Hunter, 1987; Periañez and Elliott, 2002):

$$D_v = \sqrt{2K_v\Delta t}, \quad (6)$$

148 which can be given towards the sea surface or bottom. Parameters used in the model and  
149 the considered particle sizes will be described below.

### 150 2.1.2 Bed load

151 A number of equations to describe bed load transport exist in literature (a brief review  
152 may be seen in Camenen and Larson, 2005). However, they are based upon a bed load  
153 transport rate not suitable for a Lagrangian description. Consequently, the approach by  
154 Bilgili et al. (2003) has been adopted, which can be directly used in a Lagrangian frame-  
155 work. In this approach, the critical flow velocity defining when the sediment movement  
156 starts is:

$$V_{cri} = 1.4\sqrt{gd_{50}} \ln \sqrt{\frac{h}{7d_{50}}} \left( \frac{d_{max}}{d_{50}} \right)^{1/7} \quad (7)$$

157 where  $h$  is a characteristic water depth,  $g$  is acceleration due to gravity,  $d_{50}$  is the mean  
158 sediment diameter and  $d_{max}$  is the maximum one. Instead of using a characteristic depth,  
159 this has been replaced by the local water depth, thus  $h = H(x, y)$ , since water depths  
160 change in more than one order of magnitude over the model domain. Above the critical

161 velocity, particles are assumed to travel at one-sixth of the depth averaged current (Bilgili  
162 et al., 2003). If the current decreases below  $V_{cri}$  the particle stops its movement. A two-  
163 way linear interpolation method is used to evaluate water velocity at each particle position  
164 from the four nearest points to the particle where the hydrodynamic model provides values  
165 for the water velocity (Clarke, 1995).

## 166 2.2 Hydrodynamic conditions

167 The hydrodynamic model provides the horizontal water currents  $(u, v)$  and water depths  
168  $H$  over the domain, which are required to force the sediment transport model. It is  
169 described in detail in Periañez and Abril (2015). Essentially, it is a two-dimensional  
170 depth-averaged hydrodynamic model which solves the equations for mass and momentum  
171 conservation.

172 The computational grid has been obtained from GEODAS database, available on-  
173 line, with a resolution of 4 minutes of arc, both in longitude and latitude. It extends  
174 from 29°N to 46°N and from 6°W to 37°E, thus covering the entire Mediterranean. It is  
175 worth noting that a higher spatial resolution also requires a smaller time step and thus  
176 a computational cost which can hardly be afforded to study the entire Mediterranean.  
177 Limiting the study area to the Alboran Sea or to the Western Mediterranean has the  
178 problem of providing reliable boundary conditions at the eastern open boundary, which  
179 affects the water circulation pattern. Furthermore, and as shown further in this work, a  
180 not negligible fraction of suspended load is able to reach the eastern Mediterranean basin.

181 To simulate the Messinian sea level, the base level of the present day bathymetry was  
182 dropped to -2400 m. This value was selected since the equilibrium level of the isolated  
183 Mediterranean was between 1500 and 2700 m below present sea level, according to Blanc  
184 (2006). It was used in our hydrodynamic simulations presented in Periañez and Abril  
185 (2015). The Messinian coastline obtained in this way is shown in Fig. 1B (red line). It



186 compares well with the provided by Loget et al. (2005), indicated by the limit in the  
187 Messinian evaporites in their paper.

188 Although this is an approximation to the Messinian topography, target model results  
189 attain for the likely conditions of peak flow at the Strait of Gibraltar (i.e., when water  
190 level at the Mediterranean was about 170 m below the Atlantic level, according to Abril  
191 and Periañez, 2016). This can be clearly seen in Fig. 2, where time evolution of water flow  
192 through the Strait of Gibraltar, depth of the eroded sill and Mediterranean sea level are  
193 presented from the previous calculations. The shaded area indicates the maximum flow  
194 conditions. For these conditions, the accurate reconstruction of the Messinian bathymetry  
195 is expected to be less influencing. The goal of this 2D 4-arc-minutes model is to generate  
196 a reliable water circulation for the whole Mediterranean consistent with the water inflow  
197 at peak-flow conditions predicted by the higher resolution model by Abril and Periañez  
198 (2016) developed for the Strait of Gibraltar and the western Mediterranean.

199 Instead of simulating sediment transport along the whole flood duration, currents  
200 obtained during the peak flow at Gibraltar have been used. This is the moment when  
201 maximum erosion is produced and sediments are transported to longer distances. More-  
202 over, it is not computationally feasible to simulate particle transport during the whole  
203 filling period. The peak flow is about 70 Sv (Fig. 2) and corresponding currents are about  
204 50 m/s in the Strait of Gibraltar (Periañez and Abril, 2015). A zoom of water depths and  
205 currents at this stage in the most western part of the Mediterranean may be seen in Fig.  
206 3. The general circulation pattern obtained in the whole Mediterranean Sea can be seen  
207 in Fig. 4. The horizontal and vertical diffusion coefficients (equations 2 and 3) resulting  
208 at this moment from the circulation in Fig. 4 are presented in Fig. 5. These diffusion  
209 coefficients are required to solve sediment transport.

210 As an example, the time evolution of the computed bed stresses over the domain may  
211 be seen in Electronic Supplementary Material. Bed stress is an essential factor to define  
212 the regions where deposition may occur.

	Size ( $\mu\text{m}$ )	$\tau_{cd}$ ( $\text{N/m}^2$ )	$w_s$ ( $\text{m/s}$ )
Clay	1	0,06	$3,14 \times 10^{-6}$
Silt	15	0,08	$7,07 \times 10^{-4}$
Fine sand	63	0,1	$3,24 \times 10^{-3}$
Medium sand	500	0,25	$5,78 \times 10^{-2}$
Coarse sand	1000	0,5	$8,10 \times 10^{-2}$

Table 1: Characteristics of the sediment classes used to simulate suspended load transport.

	$d_{50}$ ( $\mu\text{m}$ )	$d_{max}$ ( $\mu\text{m}$ )
Granule	4000	8000
Pebble	32000	46000
Cobble	87000	128000

Table 2: Characteristics of the sediment classes used to simulate bed-load transport.

## 2.3 Model parameters driving sediment transport

Sediment particles transported in suspension are released in the Strait of Gibraltar, just downstream the sill and homogeneously distributed over the transversal section of the strait. Five characteristic sizes have been simulated according to the Wentworth scale (Open University Team, 2005). These sediment classes are given in Table 1. 20000 particles are released for each class.

Settling velocity for the two smallest grains are calculated from Stokes's law. In the case of sands, experimental curves which give the settling velocity vs. grain size have been used (Eisma, 1993; Ji, 2008). It is known (see for instance Tattersall et al., 2003) that the critical deposition stress for cohesive sediments typically ranges between 0,04 and 0,1  $\text{N/m}^2$ . For non cohesive sediments, observations in natural systems indicate that 100  $\mu\text{m}$  sands are transported in suspension for stresses typically exceeding 0,1  $\text{N/m}^2$  (Open University Team, 2005). This critical stress increases with particle size, being in the order of 0,5  $\text{N/m}^2$  for 1000  $\mu\text{m}$  sands. Consequently, the values indicated in Table 1 for the critical deposition stresses may be considered realistic.

Three sediment classes have been considered to simulate bed-load transport. Their characteristics are presented in Table 2, again according to the Wentworth scale. It must be noted that the giant jet of Atlantic waters could have displaced blocks of greater sizes, but their transport should have remained confined within the bounds defined by the computed transportation for the cobble fraction. In these simulations, particles of each class are homogeneously distributed over the seabed of the whole Strait of Gibraltar, from  $-6^\circ$  to  $-5.3^\circ$  longitude. Then  $V_{cri}$  (Eq. 7) and water velocity at each particle position are compared to evaluate whether the particle moves.

## 3 Results and discussion

### 3.1 Suspended load

In the case of suspended load, the position of particles sedimented for each grain size are presented in Fig. 6. These results correspond to a 20 day long simulation, from the moment when particles are released in the Strait of Gibraltar. Longer simulations have been carried out, but results remain essentially the same. Indeed, histograms representing the number of deposited particles as a function of time are presented in Fig. 7 for each particle class. A “clock” is attached to each particle to obtain this information. The clock starts running when the particle is released and it is stopped when deposited. It may be seen that most particles fall on the seabed within the first 10 days after release. Also, it may be noted that the smallest number of sedimented particles is found for clays (7190). These are the smallest particles, with the lowest settling velocity and which are easily kept in suspension by turbulence. Although only 36 % of the released clay particles are deposited, particles remaining in suspension are subjected to a strong turbulent diffusion. This implies that particles will be rather mixed through the Mediterranean and will hardly give place to noticeable deposits once that they eventually fall on the seabed.

252       Returning to Fig. 6, as the particle size increases, and thus the settling velocity,  
253 particles fall on the seabed closer to the Strait of Gibraltar. But, independently from  
254 this, paths followed by the different particle classes are determined by water circulation  
255 and thus are the same.

256       There are regions of particle deposition, for all sizes, at both north and south sides of  
257 the Strait of Gibraltar connection with the Alboran Sea. These regions are related to the  
258 low water velocity (and thus low bed stress, which allows deposition) apparent in these  
259 areas (Fig. 3). An eddy is formed in the central Alboran Sea. This eddy is apparent in  
260 the water current magnitude map in Fig. 3 and is related to the topography of the basin  
261 (same figure), with larger water depths here. The low bed stress in the center of the eddy  
262 allows particle deposition for all classes except for clays (Fig. 6). There are also regions of  
263 deposition at the connection of the Alboran Sea with the western Algerian Basin. These  
264 will be commented below. Then particles follow two main routes, one along the African  
265 coast and the second south of the Balearic Islands and Sardegna. A small fraction of  
266 sediments, except for the coarse sand, reach the eastern Mediterranean through the Sicily  
267 Strait.

268       Maps in Fig. 6 only show the final position of particles once they fall on the seabed,  
269 but do not allow to deduce which are the regions of higher or lower deposition. This  
270 information can be obtained from the density of deposited particles per unit surface of  
271 the seabed. Theoretically, it is possible to assign a mass to each particle and then to  
272 evaluate deposition at each point in terms of mass per unit surface and time and/or  
273 length/time. However, we do not know the sediment mass of each class which has been  
274 eroded from the Strait of Gibraltar. Even if this mass could be estimated, we do not know  
275 how long such erosion lasted, i.e., it did not occur in the 20 day interval which has been  
276 simulated.

277       Consequently, the density of particles per unit surface has been evaluated and then  
278 normalized to the maximum value. This allows, at least, quantitative comparisons of

regions of low and high sedimentation. This information is presented in Fig. 8, where the red color indicates areas of higher deposition than the blue color. The areas of largest deposition are both shores of the Alboran Sea, at its connection to the Strait of Gibraltar. These are regions of low water velocity, as can be seen in Fig. 3. Significant deposition also occurs in the southeast Spanish coast, which is also a low current area, and in the central Alboran Sea, about  $36^{\circ}\text{N}$  and  $-2.5^{\circ}\text{W}$ . Currents in this area are weak, which is due to a sudden increase in water depths (Fig. 3). South from this region, the area to the east of present-day Cape Tres Forcas is protected from the jet flowing out the Alboran Sea at about  $35.5^{\circ}\text{N}$  (Fig. 3) and particles are deposited in the zone.

Although the density of particles is smaller than in the regions of the Alboran Sea mentioned above, very extensive deposits of mainly silts and fine sands are apparent between the Balearic Islands and Sardegna. As may be seen in the current distribution in Fig. 3, water flowing into the Mediterranean follows two pathways: the main curves to the south as leaving the Alboran Sea and then follows the African shore. The second, with weaker current, flows in an almost parallel trajectory to the former reaching the south of the Balearic Islands. These jets are the vectors of particles, which are deposited along their paths according to the corresponding settling velocity and critical deposition stress. This is apparent in Fig. 8 for all classes except clays. Deposition does not occur in the weak-current region between both jets because particles are not significantly being introduced into this area; they remain in the jets.

Thus, generally speaking, particles are deposited in regions of low current (and thus low bed stress); which appear due to a sudden increase in water depth (as in the central Alboran Sea) or because the area is protected from the intense jets (opening of the Strait of Gibraltar and connection Alboran Sea-Western Mediterranean). In addition, particles fall on the seabed along the path of the jets which transport them. Depending on the particle size (and thus settling velocity), they may reach longer distances. Very low deposition occurs for clays, because they are easily maintained in suspension by turbulence. The more

306 extensive deposits in the western Mediterranean may be expected first for fine sands and  
307 second for silts. Medium and coarse sands fall down mainly within the Alboran Sea.

## 308 **3.2 Bed load**

309 Results of the simulations for bed load are shown in Fig. 9. Only the final positions of  
310 particles which have moved have been plotted in this figure. Particles which have stayed  
311 at rest during all the simulation have been discarded. Bed-load transport is entirely  
312 determined by the water current, thus all classes are moved by the strong jet leaving the  
313 Strait of Gibraltar. Pebbles and cobbles remain close to the Strait, not reaching longitudes  
314 eastwards from  $-4^{\circ}\text{W}$ . In contrast, granules are transported to a longer distance by this  
315 jet, reaching the area north from the present-day Alboran Island and even to the east of  
316 this region (see the current path in Fig. 3). Since turbulent diffusion does not exist for  
317 bed-load transport, all particles follow the water streamlines, as it is apparent in Fig. 9.  
318 This fact implies that deposits of coarse sediments eroded from the Strait of Gibraltar  
319 and transported as bed-load are much more localized in space along water streamlines  
320 than deposits of material transported in suspension.

321 Seismic records evidence the presence of deposits resting on one of the channelized  
322 erosive surface of the Zanclean channel system, in the eastern Alboran Sea (Estrada et al.,  
323 2011) (see Fig. 10). They have an along-channel patchy distribution, and their locations  
324 match with the flood jet path deduced by the numerical model (compare Figs. 3 and 10).  
325 Acoustically, these deposits are easy to identify in the seismic records by their contrasting  
326 acoustic features. They are characterized by chaotic and hyperbolic echoes with reflections  
327 of high amplitude which define irregular bodies up to 208 m thick, 35 km long and 7 km  
328 wide (Fig. 10). The recent high-resolution Plio-Quaternary seismic stratigraphy defined  
329 in the Alboran Sea (Juan et al., 2016) confirms a Zanclean age for those deposits. In fact,  
330 they are topped by well-layered Pliocene sediments deposited in deep marine conditions

(Juan et al., 2016). Based on their chronology, location, distribution and nature of the overlying Pliocene sediments, all suggest the Zanclean deposits may represent sediments transported and deposited under the action of the Zanclean flooding. In addition, their lithoseismic attributes suggest that they represent coarse sediments deposited in relatively high-energy conditions, coinciding then with those areas of high density of sand particles deduced by the numerical model (Fig. 8). The patchy distribution displayed by the Zanclean flood deposits has been also described in other megaflood deposits (e.g., Altai megaflood, Carling et al., 2009).

## 4 Conclusions

A numerical model which simulates both suspended and bed-load sediment transport during the Zanclean flood of the Mediterranean has been developed. The hydrodynamics has been obtained from a computational fluid dynamic model previously developed by the authors and applied to the Zanclean flood. The model was solved for the peak flow conditions under which erosion of the greater part of the former Gibraltar divide takes place. The sediment transport model works in a Lagrangian framework. Paths of sediment particles eroded from the Strait of Gibraltar during the flood are calculated until these particles are deposited on the seabed. Thus, the regions where Zanclean deposits could be present have been determined. Because of the poorly constrained geography of the Mediterranean during the Late Miocene, the use of these results to predict locations with accumulated sediment accumulations must be done with caution. Nevertheless, results provide some valuable clues with respect to the distance travelled by the sediments and the areas where deposits could be searched, as Zanclean chaotic deposits identified on seismic profiles in the Eastern Alboran Basin indicate; and/or areas which could be discarded in any attempt to find such Zanclean deposits.

The post-flood distributions of sediment transported in suspension and bed-load have

356 been obtained. In the case of suspended load, particles are deposited in regions of low  
357 water currents, i.e., low bed stress. These regions are related to zones sheltered from  
358 the water jet incoming the Mediterranean by local topography, areas where a sudden  
359 increase of water depth occur and the center of eddies. Thus, main deposits could be  
360 present at both sides of the Strait of Gibraltar (i.e., both sides of the erosion channel),  
361 the center of the Alboran Sea and at both north and south sides of the Alboran Sea, at its  
362 connection with the Mediterranean. Of course, particles transported with the main jet fall  
363 according to their settling velocity and are finally deposited on the seabed. The distance  
364 of these deposits to the Strait of Gibraltar increases as particle size decreases, as could  
365 be expected. Thus, very extensive deposits of mainly silts and fine sands appear between  
366 the Balearic Islands and Sardegna. Long deposits are also apparent along Algeria coast.  
367 Sediment particles transported as bed-load follow streamlines, since turbulent mixing does  
368 not act. Thus, deposits of very coarse sediment eroded from the Strait of Gibraltar and  
369 transported as bed-load should be more localized in space than finer grain deposits.

370 Sedimentary register on seismic records in the eastern Alboran Sea are consistent with  
371 the presence of such deposits that display a patchy distribution along the bottom of the  
372 Zanclean erosion channel and on its flanks.

373 Sediment in suspension is transported towards the east to distances reaching some  
374 2000 km in the case of clay and silt; and reaching some 1000 km in the case of coarse  
375 sand. In contrast, coarser sediment transported as bed load stays closer to the Strait of  
376 Gibraltar. Maximum travelled distances are of the order of some 500 km for granule and  
377 reduce to some 100 km for cobble.

## 378 5 References

379 Abril, J.M., Periáñez, R., 2016. Revisiting the time scale and size of the Zanclean  
380 flood of the Mediterranean (5.33 Ma) from CFD simulations. *Marine Geology* 382,



242-256.

Bilgili, A., Swift, M.R., Lynch, D.R., Ip, J.T.C., 2003. Modelling bed-load transport of coarse sediments in the Great Bay Estuary, New Hampshire. *Estuarine, Coastal and Shelf Science* 58, 937-950.

Blanc, P.L., 2006. Improved modelling of the Messinian Salinity Crisis and conceptual implications. *Palaeogeography, Palaeoclimatology, Palaeoecology* 238, 349-372.

Camemen, B., Larson, M., 2005. A general formula for non-cohesive bed load sediment transport. *Estuarine, Coastal and Shelf Science* 63, 249-260.

Carling, P.A., Martini, P., Herget, J., Borodavko, P., Parnachov, S., 2009. 13 Megaflood sedimentary valley fill: Altai Mountains, Siberia. In: Devon M. Burr, Paul A. Carling and Victor R. Baker (Editors) *Megaflooding on Earth and Mars* pp. 243-264. Cambridge University Press, UK.

Clarke, S., 1995. Advective/diffusive processes in the Firth of Forth. PhD Thesis, University of Wales, Bangor, UK.

Cushman-Roisin, B., Beckers, J.M., 2011. *Introduction to Geophysical Fluid Dynamics*. Elsevier.

Eisma, D., 1993. *Suspended Matter in the Aquatic Environment*. Springer-Verlag, Berlin.

Esteras, M., Izquierdo, J., Sandoval, N.G., Bahmad, A., 2000. Evolución Morfológica y Estratigráfica Pliocuaternaria del Umbral de Camarinal (Estrecho de Gibraltar) Basada en Sondeos Marinos. *Rev. Soc. Geol. España* 13, 539-550.

Estrada, F., Ercilla, G., Gorini, Chr., Alonso, B., Vázquez, J.T., García-Castellanos, D., Juan, C., Maldonado, A., Ammar, A., Elabbassi, M., 2011. Impact of pulsed

Atlantic water inflow into the Alboran Basin at the time of the Zanclean flooding.  
Geo-Marine Letters 31, 361-376.

García-Castellanos, D., Villaseñor, A., 2011. Messinian salinity crisis regulated by  
competing tectonics and erosion at the Gibraltar arc. Nature Letters 480, 359-363.

García-Castellanos, D., Estrada, F., Jiménez-Munt, I., Gorini, C., Fernández, M.,  
Vergés, J., De Vicente, R., 2009. Catastrophic flood of the Mediterranean after the  
Messinian salinity crisis. Nature 462, doi: 10.138/nature08555.

Hsü, K.J., Cita, M.B., Ryan, W.B.F., 1973. The origin of the Mediterranean evap-  
orites. In: Ryan, W.B.F., Hsü, K.J., Cita, M.B. (Editors) *Initial Reports of the  
Deep Sea Drilling Project 13*, US Government Printing Office, Washington DC. pp.  
1203-1231.

Hunter, J. R., 1987. The application of Lagrangian particle tracking techniques  
to modelling of dispersion in the sea. In: J. Noye (Ed.), *Numerical modelling.  
Applications to marine systems*. pp. 257-269. Elsevier, North-Holland.

Ji, Z.G., 2008. *Hydrodynamics and Water Quality. Modeling Rivers, Lakes and  
Estuaries*. Wiley, New Jersey.

Juan, C., Ercilla, G., Hernández-Molina, F.J., Estrada, F., Alonso, B., Casas, D.,  
García, M., Farran, M., Llave, E., Palomino, D., Vázquez, J.T., Medialdea, T.,  
Gorini, C., D'Acremont, E., El Moumni, B., Ammar, A., 2016. Seismic evidence  
of current-controlled sedimentation in the Alboran Sea during the Pliocene and  
Quaternary: palaeoceanographic implications. Marine Geology 378, 292-311.

Lane, A., 2005. Development of a Lagrangian sediment model to reproduce the  
bathymetric evolution of the Mersey Estuary. Ocean Dynamics 55, 541-548.

Loget, N., Driessche, J.V.D., Davy, P., 2005. How did the Messinian Salinity Crisis end? *Terra Nova* 17, 414-419.

Martín, J.M., Braga, J.C., Betzler, C., 2001. The Messinian Guadalhorce corridor: the last northern, Atlantic-Mediterranean gateway. *Terra Nova* 13, 418-424.

Open University Team, 2005. *Waves, Tides and Shallow Water Processes*. Butterworth-Heinemann, Oxford.

Periáñez, R., Elliott, A.J., 2002. A particle tracking method for simulating the dispersion of non conservative radionuclides in coastal waters. *Journal of Environmental Radioactivity* 58, 13-33.

Periáñez, R., Abril, J.M., 2015. Computational fluid dynamics simulations of the Zanclean catastrophic flood of the Mediterranean (5.33 Ma). *Palaeogeography, Palaeoclimatology, Palaeogeography* 424, 49-60.

Proctor, R., Flather, R. A., Elliott, A. J., 1994. Modelling tides and surface drift in the Arabian Gulf: application to the Gulf oil spill. *Continental Shelf Research* 14, 531-545.

Proehl, J.A., Lynch, D.R., McGillicuddy, D.J., Ledwell, J.R., 2005. Modeling turbulent dispersion on the North Flank of Georges Bank using Lagrangian particle methods. *Continental Shelf Research* 25, 875-900.

Roveri, M., Flecker, R., Krijgsman, W., Lofi, J., Lugli S., Manzi, V., Sierro, F.J., Bertini, A., Camerlenghi, A., De Lange, G., Govers, R. Hilgen, F.J., Hübscher, Chr., Meijer, P.Th., Stoica, M., 2014. The Messinian Salinity Crisis: Past and future of a great challenge for marine sciences. *Marine Geology* 352, 25-58.

Ryan, W.B.F., 2009. Decoding the Mediterranean salinity crisis. *Sedimentology* 56, 95-136.

451 Tattersall, G.R., Elliott, A.J., Lynn, N.M., 2003. Suspended sediment concentra-  
452 tions in the Tamar estuary. *Estuarine, Coastal and Shelf Science* 57, 679-688.

453      **Caption to Electronic Supplementary Material**

454      **ESM 1.** Temporal evolution of the computed bed stress magnitude (Pa) along the  
455 Zanclean flood in logarithmic scale. The red line is the present-day 2400 m isobath.

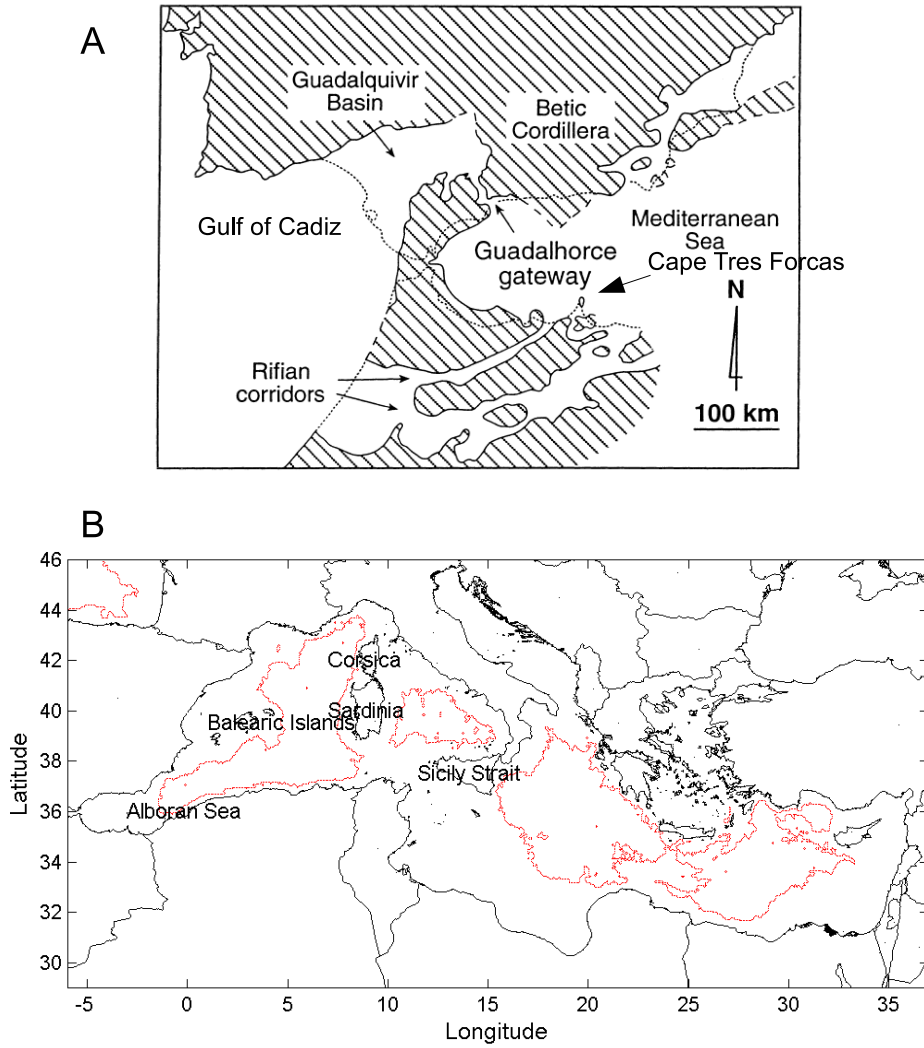


Figure 1: A: Western Mediterranean palaeogeography during the early Messinian (Martín et al., 2001). B: Map of the computational domain showing geographic names mentioned in the text and present day (black) and Messinian (red) coastlines according to the Limit of the Messinian evaporites (Loget et al., 2005).

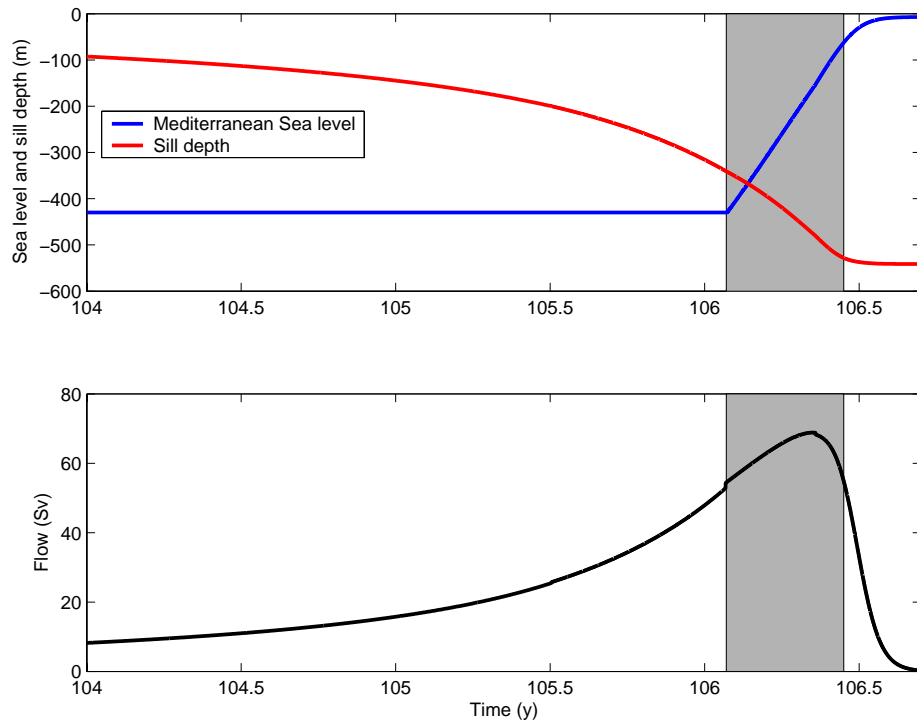


Figure 2: Computed (Abril and Periañez, 2016) time evolution of water flow, depth of the eroded sill in Gibraltar and Mediterranean Sea level (measured downwards from the Atlantic Ocean level) along the flood process. The shaded box indicates maximum flow conditions.

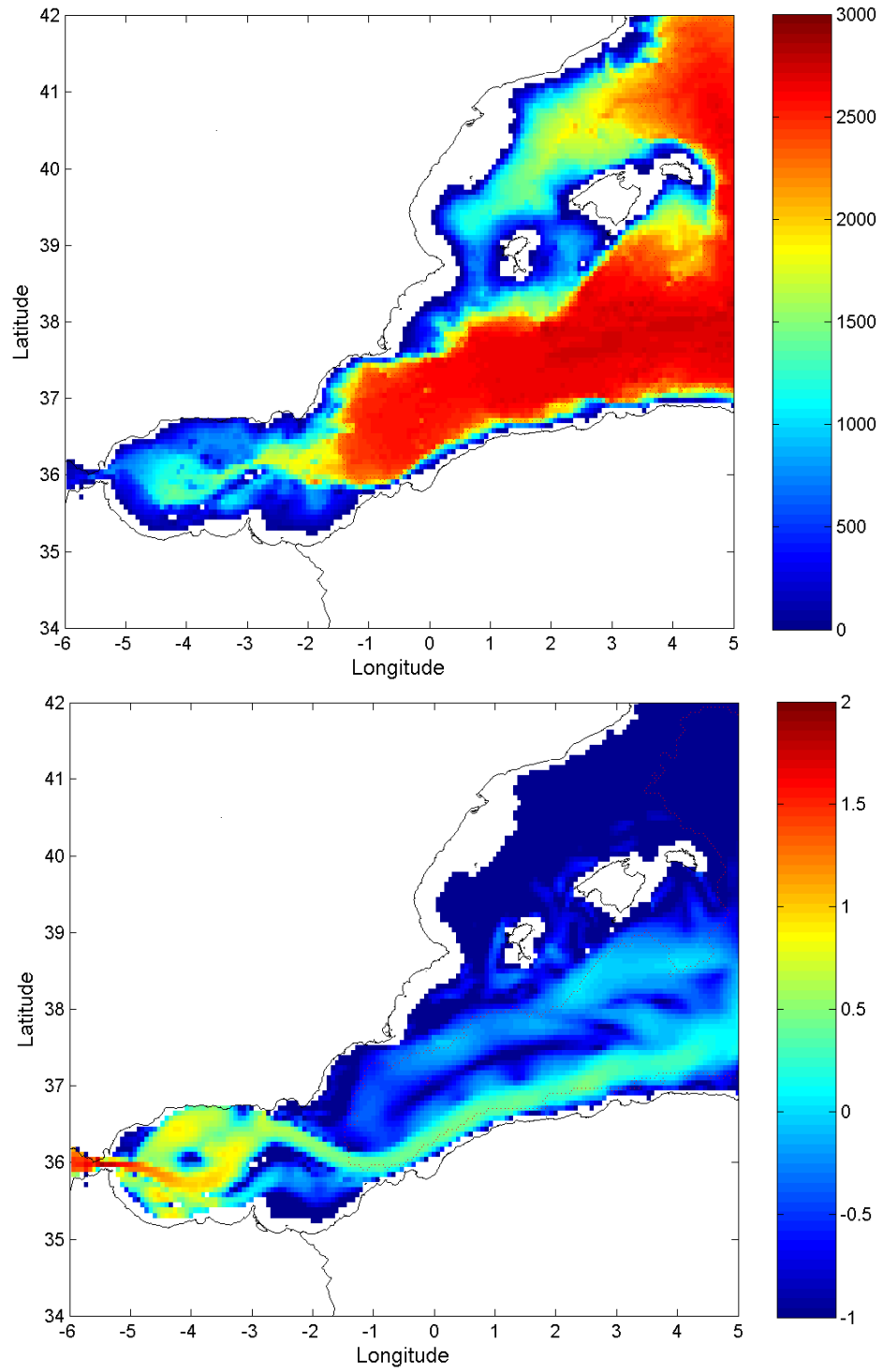


Figure 3: Zoom in the western Mediterranean at the considered stage of flooding. Top: water depths (m). Bottom: water current magnitude (m/s) in logarithmic scale.



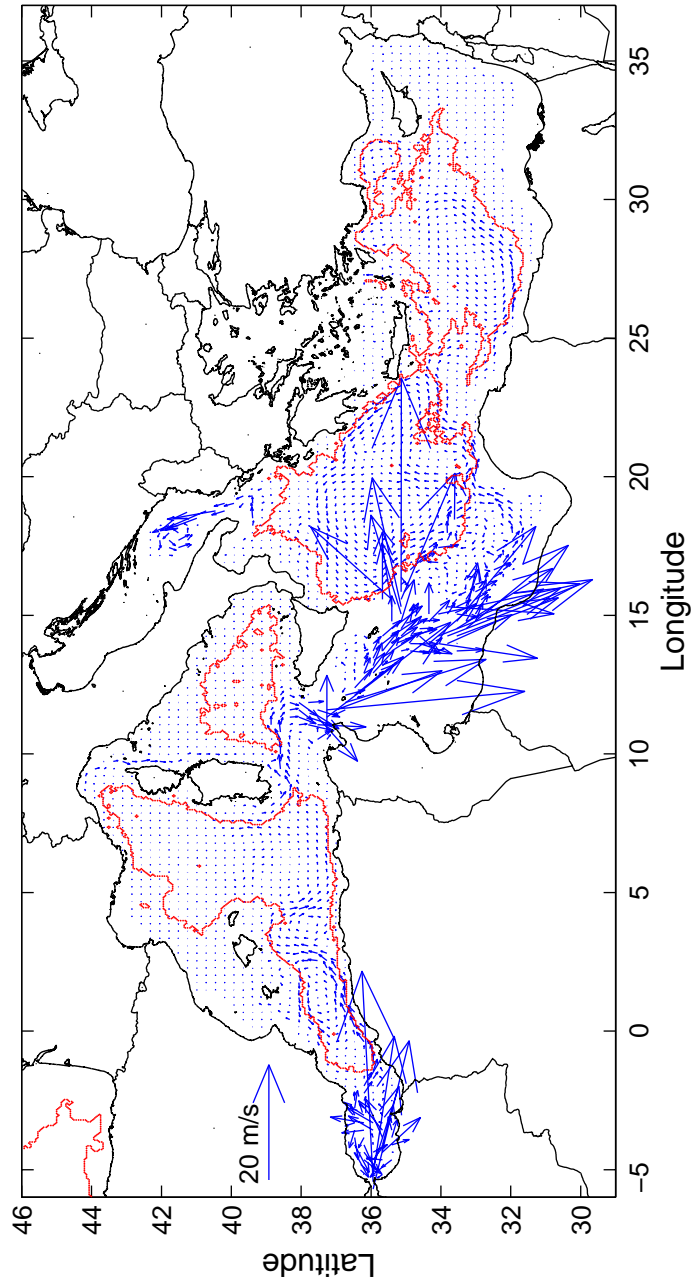


Figure 4: Current field calculated in the Mediterranean at peak flow conditions. Only one of each 16 calculated vectors is drawn for more clarity. The red line indicates the Messinian coastline.

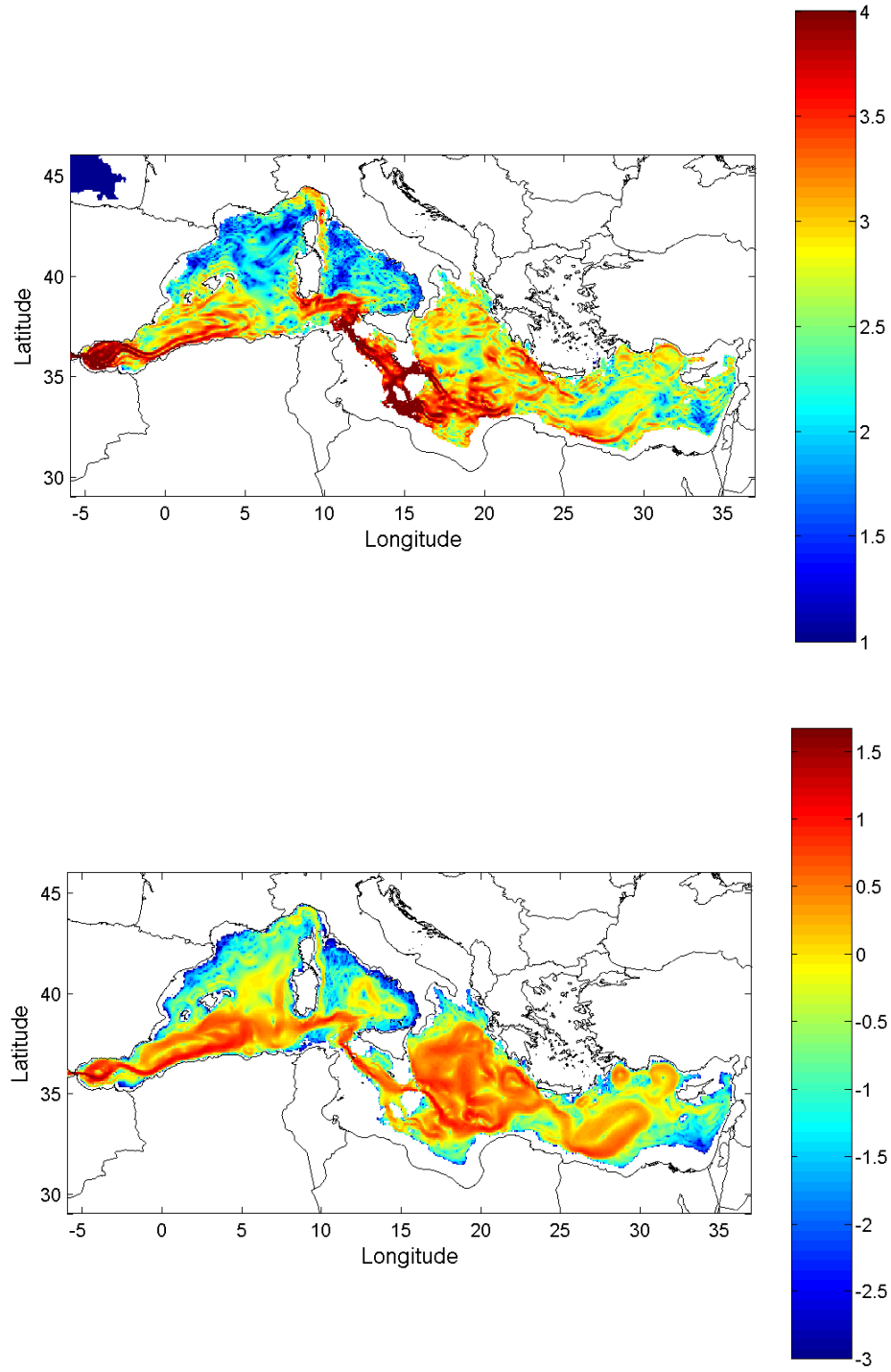


Figure 5: Horizontal (top) and vertical (bottom) diffusion coefficients ( $\text{m}^2/\text{s}$ ) resulting from water circulation during peak flow conditions (Fig. 4) in logarithmic scale. The present-day coastline is shown.

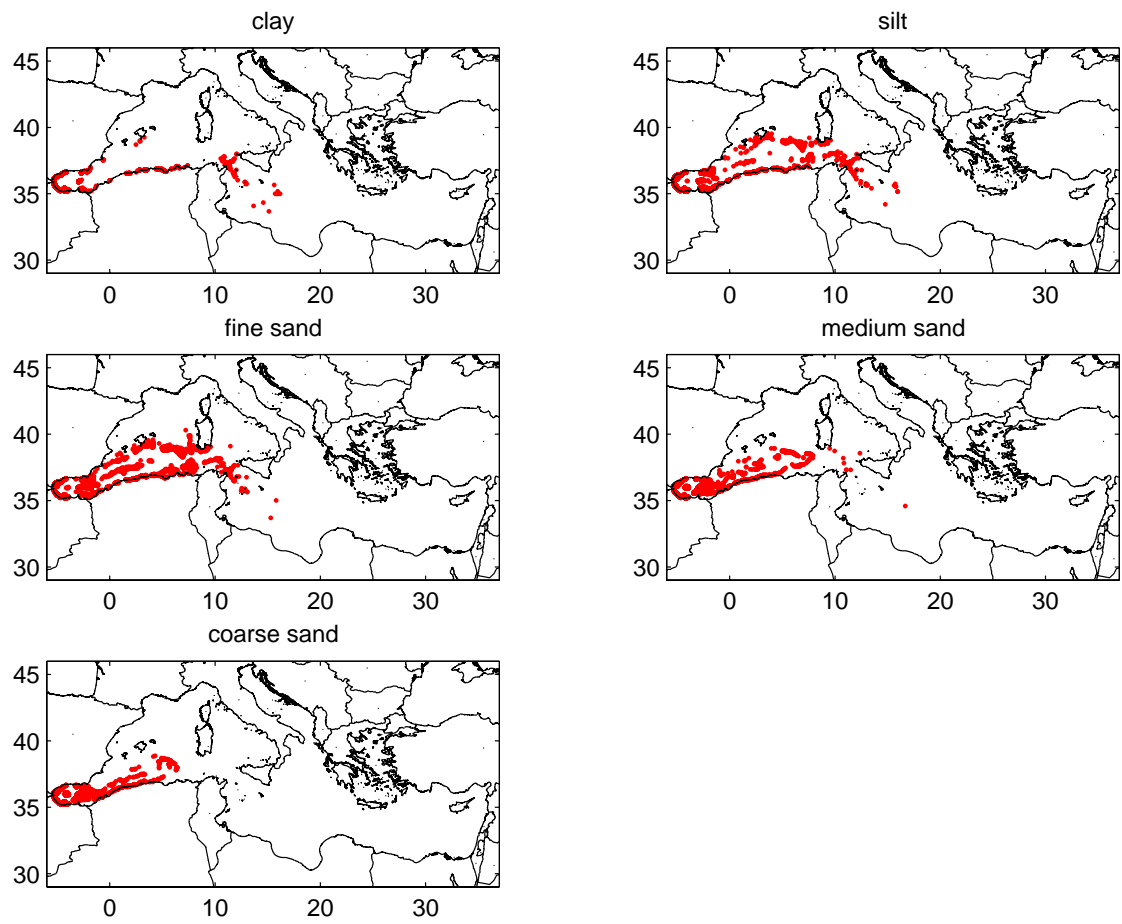


Figure 6: Locations of particles transported in suspension when they are sedimented and thus stop their movement.

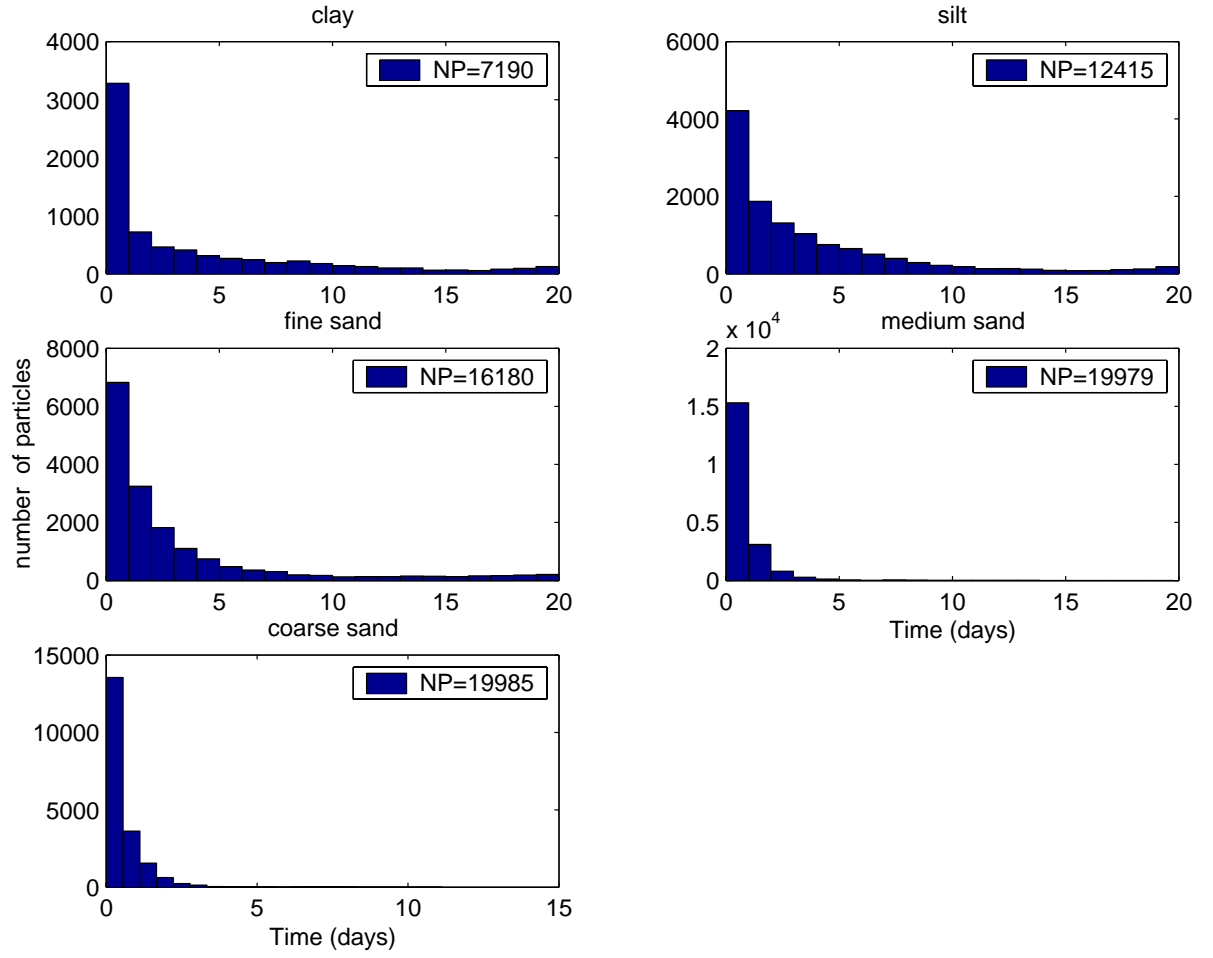


Figure 7: Histograms showing the ages of deposited particles for each class. The total numbers of deposited particles (NP) are indicated (20000 particles of each class are released).

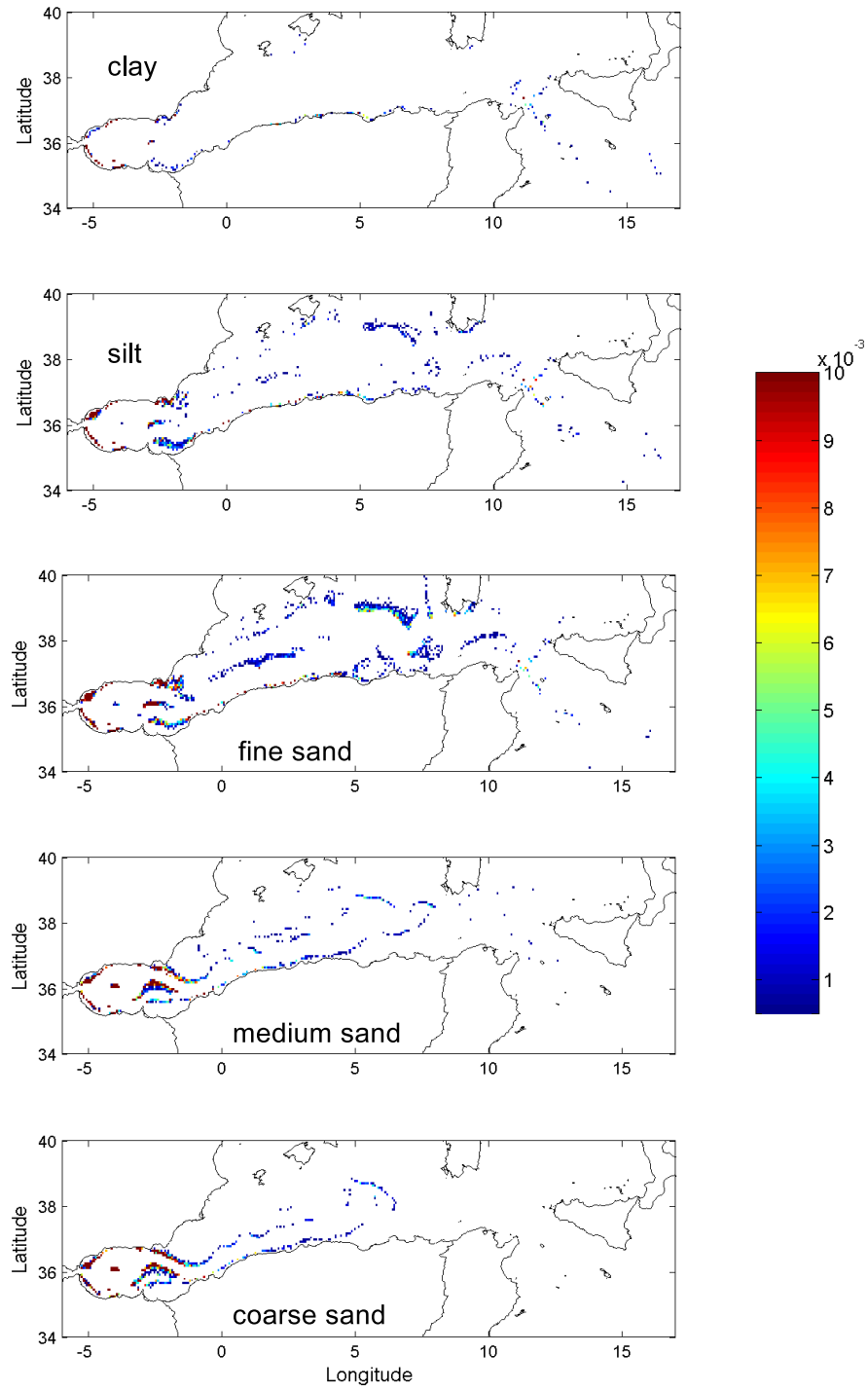


Figure 8: Density of sedimented particles per unit surface normalized to the maximum value in its class.

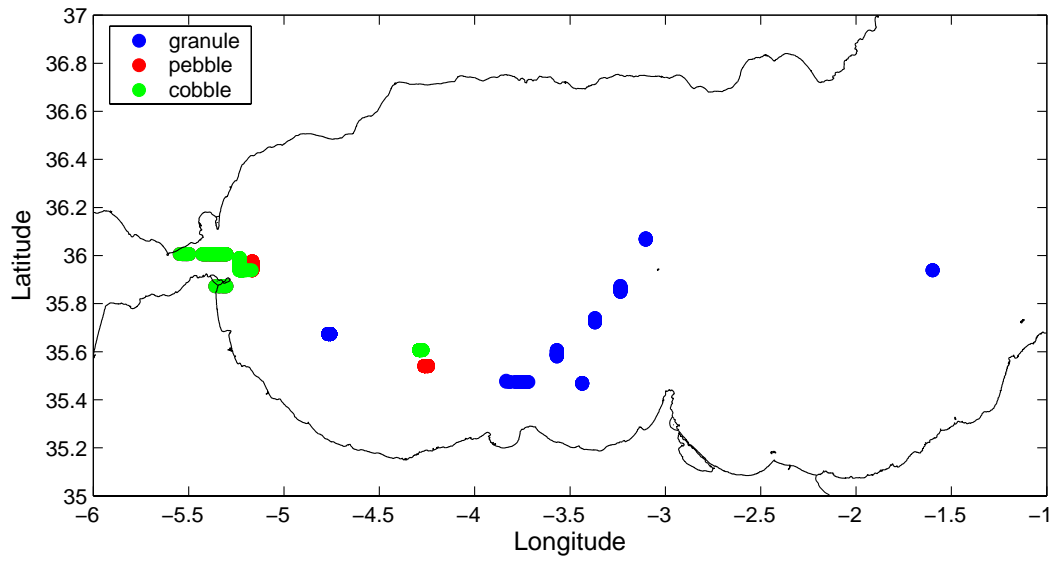


Figure 9: Final positions of particles which have been transported as bed-load.

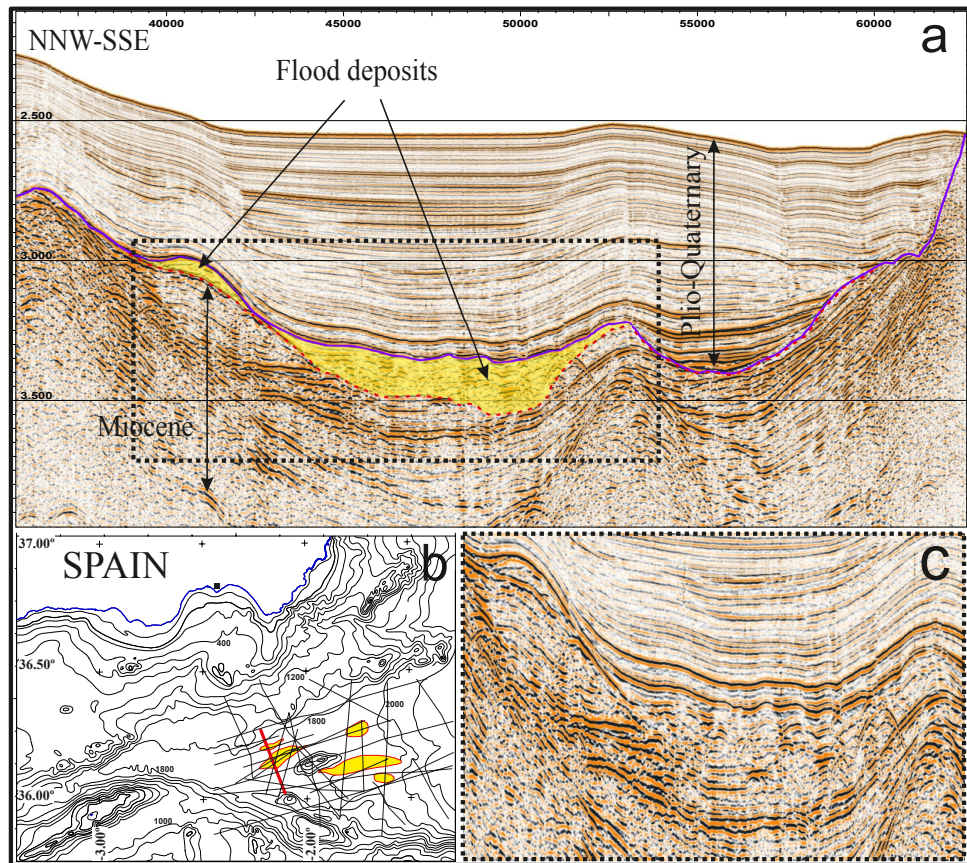


Figure 10: a) Airgun seismic profile showing flood deposits (yellow areas) resting on the Zanclean erosive channel (red dashed line). Purple line represents the base of Pliocene. b) Bathymetric map showing seismic survey, red line, and patchy distribution of flood related deposits; c) uninterpreted view of flood-related deposits. Legend: vertical scale in seconds (two way travel time); horizontal scale in meters.